Beaming light from a subwavelength metal slit surrounded by dielectric surface gratings

D. Z. Lin[1], C. K. Chang[1], Y. C. Chen[1], D. L. Yang[1], M. W. Lin[2], J. T. Yeh[2], J. M. Liu[2], C. H. Kuan[3], C. S. Yeh[1], amd C. K Lee[1, 4]

[1] *Institute of Applied Mechanics, National Taiwan University, Taipei, Taiwan*

[2] *Industrial Technology Research Institute, Material and Chemical Research Laboratories, Hsinchu, Taiwan*

[3] *Graduate Institute of Electronics Engineering and Department of Electrical Engineering, National Taiwan University, Taipei, Taiwan*

[4] *Department of Engineering Science & Ocean Engineering, National Taiwan University, Taipei, Taiwan*

cklee@mems.iam.ntu.edu.tw

Abstract: In this article, we demonstrate that a subwavelength metal slit surrounded by dielectric surface gratings possesses a directional beaming effect. We propose a surface plasmon diffraction scheme to explain the three kinds of beaming conditions. The numerical simulations of the illustrative structures undertaken used a Finite Difference Time Domain (FDTD) Method and a Rigorous Coupled Wave Analysis (RCWA) Method. Our simulations were found to be consistent and in agreement with the experimental results. In comparison with other metal structures, we find that dielectric metal structures offer better performance as well as the advantage of being able to be efficiently mass produced for large volume industrial applications.

OCIS codes: (240.6680) Surface plasmons; (050.1950) Diffraction gratings; (240.0240) Optics at surfaces.

References and Links

1. H. A. Bethe, "Theory of diffraction by small holes," Phys. Rev. **66**, 163-182 (1944).
2. H. J. Lezec, A. Degiron, E. Devaux, R. A. Linke, L. Martin-Moreno, F. J. Garcia-Vidal, T. W. Ebbesen, "Beaming light from a subwavelength aperture," Science **297**, 820–822 (2002).
3. F. J. Garcia-Vidal, L. Martin-Moreno, H. J. Lezec, T. W. Ebbesen, 'Focusing light with subwavelength aperture flanked by surface corrugations,' Appl. Phys. Lett., **83**, 4500-4502 (2003).
4. L. Martín-Moreno, F. J. Garcia-Vidal, H. J. Lezec, A. Degiron, T. W. Ebbesen, "Theory of highly directional emission from a single subwavelength aperture surrounded by surface corrugations," Phys. Rev. Lett. **90**, 167401 (2003).
5. L. B. Yu, D. Z. Lin, Y. C. Chen, Y. C. Chang, K. T. Huang, J. W. Liaw, J. T. Yeh, J. M. Liu, C. S. Yeh, and C. K. Lee, "Physical origin of directional beaming emitted from a subwavelength slit," Phys. Rev. B **71**, 041405 (2005).
6. J. Dintinger, A. Degiron, T. W. Ebbesen, "Enhanced light transmission through subwavelength holes," MRS Bulletin **30**, 381-384 (2005).
7. Z. B. Li, J. G. Tian, Z. B. Liu, W. Y. Zhou, C. P. Zhang, "Enhanced light transmission through a single subwavelength aperture in layered films consisting of metal and dielectric," Opt. Express **13**, 9071-9077 (2005). http://www.opticsexpress.org/abstract.cfm?id=86076
8. D. Z. Lin, L. B. Yu, C. K. Lee, C. S. Yeh, and C. L. Lin, "Simulation and fabrication of subwavelength structures for a nanometer feature enabled lens-less laser writers," Scanning **26**, I73-I77 (2004).
9. W. Srituravanich, N. Fang, C. Sun, Q. Luo, and X. Zhang, "Plasmonic Nanolithography," Nano Lett. **4**, 1085-1088 (2004).
10. S. Shinada, J. Hashizume, and F. Koyama, "Surface plasmon resonance on microaperture vertical-cavity surface-emitting laser with metal grating," Appl. Phys. Lett. **83**, 836-838 (2003).

#10399 - $15.00 USD Received 31 January 2006; revised 29 March 2006; accepted 30 March 2006

11. D. A. Stuart, A. J. Haes, C. R. Yonzon, E. M. Hicks, and R. P. Van Duyne, "Biological applications of localised surface plasmonic phenomenae," IEE Proc. Nanobiotechnology **152**, 13-32 (2005).

1. Introduction

Based on the diffraction theory, we know that transmission from a subwavelength aperture will be very weak and has a characteristic to diverge [1]. In 2002, researchers found that light transmission through a subwavelength aperture with surface corrugation will not diffract at all angles. This phenomenon has stimulated much interest over the years as it provides us with a possibility to steer light into a microscopic world [2]. Theorists have used Huygens's principle [3-4] and surface plasmon diffraction [5-6] to explain this beaming phenomenon. Of all previous research, all but one recent simulation [7] have studied only the metal structure. From our previous experiments [5], we found that metal has a tendency to crystallize during the deposition process which makes it difficult to use a focused ion beam (FIB) to arrive at the desired perfect shape during fabrication (Fig 1). In this article, we used a dielectric surface structure on metal (DM structure) instead of a metal surface structure on metal (MM structure) as the test structure. We then designed a series of experiments to measure the beaming phenomenon. Corresponding simulations were also performed to identify the underlying physical principles behind the beaming phenomenon of a DM structure.

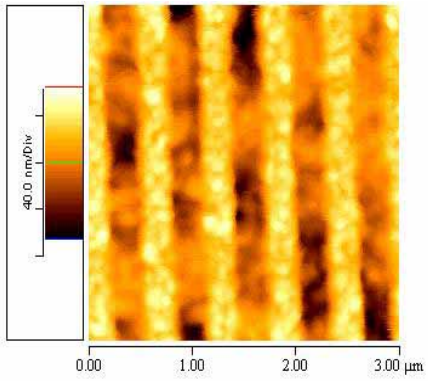

Fig.1. Atomic Force Microscope (AFM) image of a metal surface structure milled by FIB.

2. Simulation and Experimental Set-up

To further understand the details of the beaming mechanism, we first used a FDTD method to simulate the performance of the DM structure. The three simulation conditions are detailed in Fig. 2. We used three 80nm deep dielectric gratings which had a period of 465nm, 625nm, and 530nm respectively, on a 250nm thick silver film with a 230nm width slit. The incident wavelength was 633nm. Figure 3 shows the three FDTD simulation results for different periods of the DM structures of which the poynting vector S_Z is in the z-direction. Unlike metal gratings, we found that the surface plasmon (SP) does not propagate along the grating profile but penetrates through the dielectric grating and propagates along the metal and dielectric interface [Fig. 3(d)]. We defined the sign of the beaming angle to be negative when the projected direction of the diffracted beam was opposite to that of the SP propagation [5]. Similarly, a positive beaming angle indicates that the projected direction of the diffracted beam is the same as that of the SP propagation. The beaming angles shown in Fig. 3(a)~3(c) are negative, positive, and zero degree, respectively.

#10399 - $15.00 USD Received 31 January 2006; revised 29 March 2006; accepted 30 March 2006

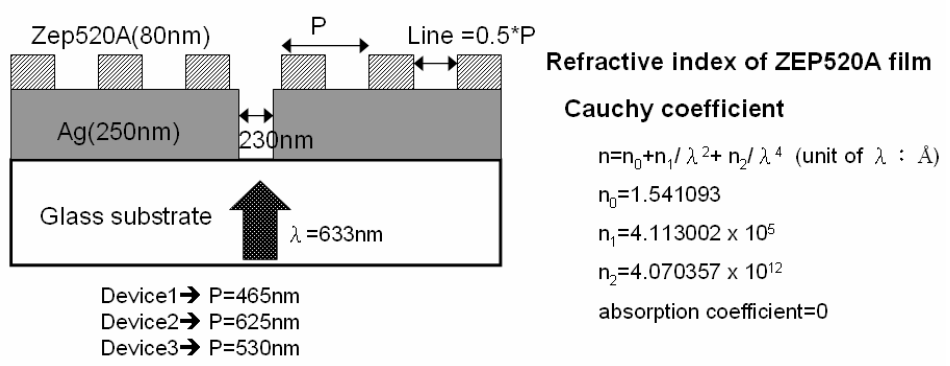

Fig. 2. FDTD simulation conditions for three DM structures. (period of Device 1 = 465m, Device 2 = 625nm and Device 3 = 530nm)

In order to verify the theoretical model, we prepared the sample under the same parameters as that of the FDTD simulations. We first evaporated 250nm silver film on a glass substrate. Then, we spin-coated an 80nm E-beam resist (ZEP520A) and used electron beam lithography (Elionix, ELS-7500EX) to fabricate the dielectric surface gratings. Finally, we used a focused ion beam (FEI, Nova 200) to mill a slit on the metal film. The final sample and SEM image are shown in Fig. 4(a). We also used an AFM (atomic force microscope) to measure the true geometry of the sample [Figs. 4(b), 4(c), and 4(d)]. The parameters are summarized in Table 1. Using the AFM, we found that the grating depth near the central slit (74nm) was shallower than that further away from the central slit (80nm). The slight difference in the grating depth may be due to the scanning image which uses an ion beam for orientation during the FIB process. Since the grating depth also highly influences the beaming angle, it is recommended that more precise geometric parameters be found before further simulations are undertaken.

In our experimental set-up, an inverted microscope (Olympus, GX71) equipped with a transmission halogen light source with a 20nm band pass color filter (central wavelength 633nm) and a polarizer (to control the TM incident wave) was used to determine the beaming angles. A series of photographs of the transmitted light were taken by a CCD camera (Olympus, DP70) by controlling the focal plane at different heights above the sample surface.

Table 1. Design and actual geometric parameters for the three devices.

Device	Design Period (nm)	Measured Period (nm)	Measured Line Width (nm)/Duty Cycle (%)	Measured Groove Depth (nm)	Simulation Beaming Angle	Experimental Beaming Angle
1	465	462.3	249.4/53.9	74	-10.77	NA
2	625	623.1	372.7/59.6	74	10.9	11.3
3	530	532.6	269.1/50.5	72	0	~0

#10399 - $15.00 USD Received 31 January 2006; revised 29 March 2006; accepted 30 March 2006

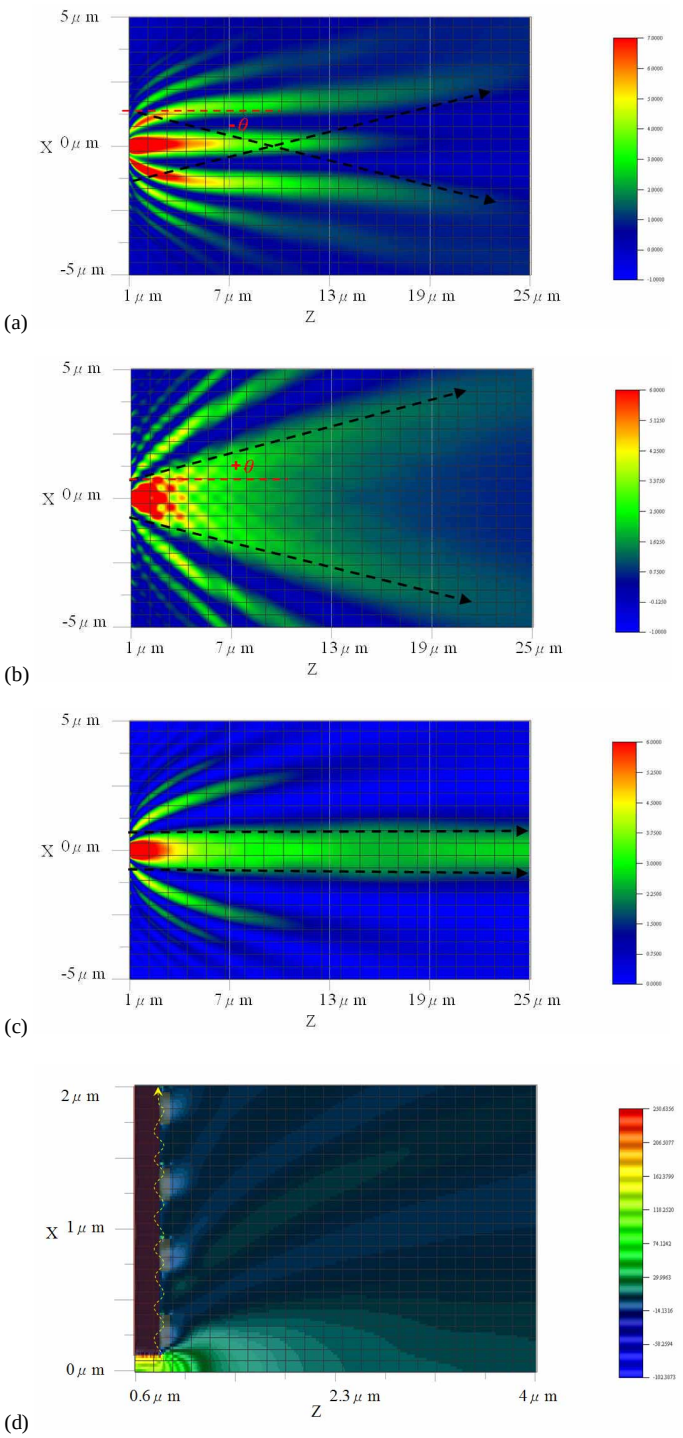

Fig. 3. FDTD simulations (Sz) of (a) Device 1 (b) Device 2 (c) Device 3 and (d) close-up view of the dielectric surface structures.

#10399 - $15.00 USD Received 31 January 2006; revised 29 March 2006; accepted 30 March 2006

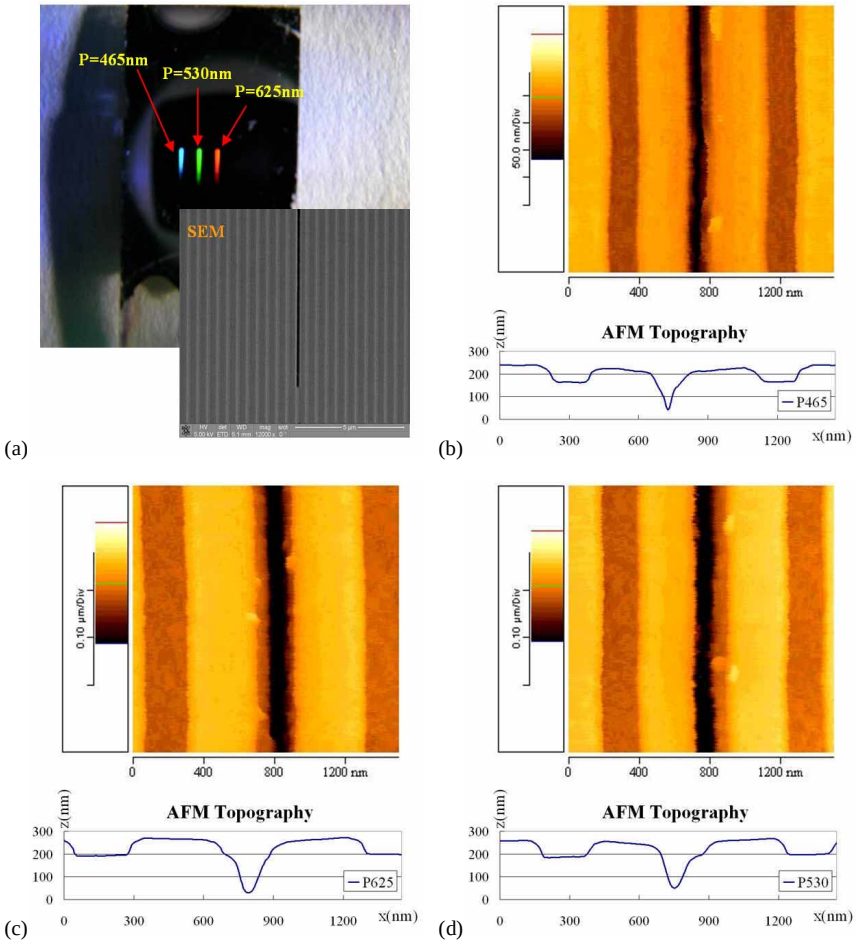

Fig. 4. (a) Picture of a prepared sample (three color band represent the three different periods of the DM structure) and AFM topography data of (b) Device 1 (P=465nm), (c) Device 2 (P=625nm), and (d) Device 3 (P=530nm).

The optical images shown in Figs. 5(a)~5(c) shows a series of images taken above the structure exit surface. All these images are two micrometer apart. We can see a white light dispersion from the data obtained, which implies that the surface plasmon is diffracted by the grating. To calculate the beaming angle, we placed a 20nm bandwidth red color filter before the sample [see Figs. 5(d)~5(f)]. We saw that for the red light in Device 1, the two crossover beams interfered with each other at the first 10μm, and then gradually separated after 15μm. For Device 2, the beaming angle of the red light was a positive angle. For Device 3, the beaming angle stayed very close to zero degree as only a very small divergence angle was observed. Taking into consideration that the experimental data was obtained using a 20 nm bandwidth red color filter and that the simulation was calculated by assuming a single wavelength of 633 nm, the FDTD simulations (Fig. 3) matched well to the experimental data.

To measure the beaming angle, we specified the lateral location (x-direction) of each cross-section (z-direction) and derived the regression lines. As the bandwidth for the color filter was not infinitesimal, we adopted an outer and inner boundary to define the central wavelength. By using the slope of the middle regression lines, the beaming angle was

#10399 - $15.00 USD Received 31 January 2006; revised 29 March 2006; accepted 30 March 2006

estimated to be 11.3 degrees for Device 2 (Fig. 6) and approximately zero degree for Device 3.

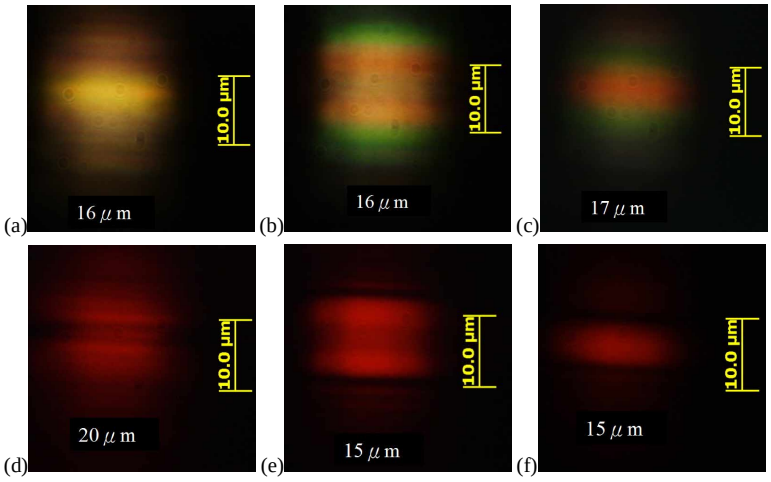

Fig. 5. Movies (low resolution~200KB & high resolution~1.7MB) of beaming phenomenon: (a) Device 1, (b) Device 2, (c) Device 3, and (d) Device 1 with filter (e) Device 2 with filter, and (f) Device 3 with filter.

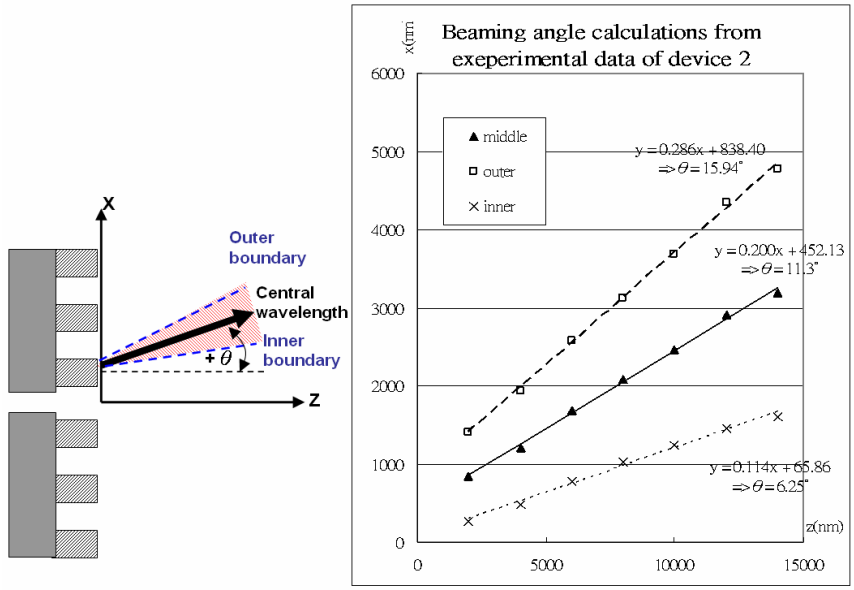

Fig. 6. Calculations of the beaming angles from experimental data of Device 2 (Fig. 5(e)). (left figure indicates the definition of the coordinates)

According to the surface plasmon diffraction theory (Eq. 1) we can calculate the beaming angle for each device. Considering the case where k_0 is the wave vector of light in free space, k_{sp} is the wave vector of the surface plasmon, Λ is the period of grating, θ is the angle of incident light, and m is integer, we can obtain

#10399 - $15.00 USD Received 31 January 2006; revised 29 March 2006; accepted 30 March 2006

$$k_{sp} \pm m\frac{2\pi}{\Lambda} = k_0 \sin\theta \ . \qquad (1)$$

However as the analytical solution of k_{sp} is difficult to derive for undulated surfaces, we instead adopted the concept of a Helmholtz reciprocal theorem and a numerical method (rigorous coupled wave algorithm, RCWA) [5]. Based on these theorems, the beaming angle can be obtained from the angles exciting the surface plasmon, i.e., resonance condition, which corresponds to a minimum reflection or maximum absorption.

Our results are shown in Fig. 7. Our theoretical predications for a 633nm incident wavelength of Device 1, Device 2, and Device 3 were -10.77 degrees, 10.9 degrees, and zero degree respectively. In Table 1, the beaming angle was obtained by calculations from the experimental data and the simulations. Since the experimental results agreed well with the simulations, it might be reasonable to conjecture that a surface plasma diffraction theory may also explain the directional beaming phenomenon of a DM structure.

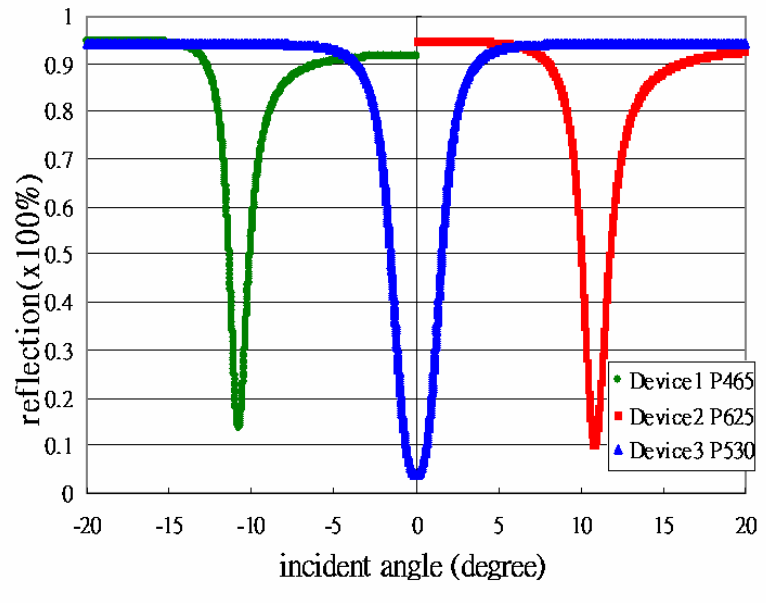

Fig. 7. RCWA simulations of resonance conditions for the three devices. Using Helmholtz reciprocal theorem, the minimum reflection (i.e. maximum absorption) indicates the beaming angle.

3. Discussion

Comparing DM structures to MM structures, we found that there are extra advantages of adopting DM structures. Firstly, the crystallization of metal on MM structures makes it difficult to mill a desired grating shape perfectly as the surface plasmon propagates along the metal grating profile. For DM structures, it propagates under the dielectric grating (see Fig.8). The observable difference between a MM and DM grating is the surface plasmon propagating path (red dotted line). A MM structure also suffers from a more intrinsic absorption and scattering by the metal which decreases the number of surface grooves on which the surface plasmon can "see" and broaden the beaming angle. Secondly, the intrinsic damping by metal on MM structures will affect the surface plasmon resonance condition. In Fig. 9, under the

#10399 - $15.00 USD Received 31 January 2006; revised 29 March 2006; accepted 30 March 2006

same geometric condition, we can see that the resonance angle of the DM structure is much sharper when compared to a MM structure. Thirdly, for mass production purposes, a DM structure is easier to be mass produced than a MM structure. There are available many tools to create a smooth dielectric thin film, such as using a spin coater, by chemical vapor deposition or with an evaporator machine. There are also many methods to fabricate dielectric surface gratings of precise shapes, such as with nano-imprints, e-beam lithography or a reactive ion etching system. Thus, with all of the above-mentioned merits for DM structures, we can see that DM structures offer a more feasible approach for industrial applications than that of MM structures.

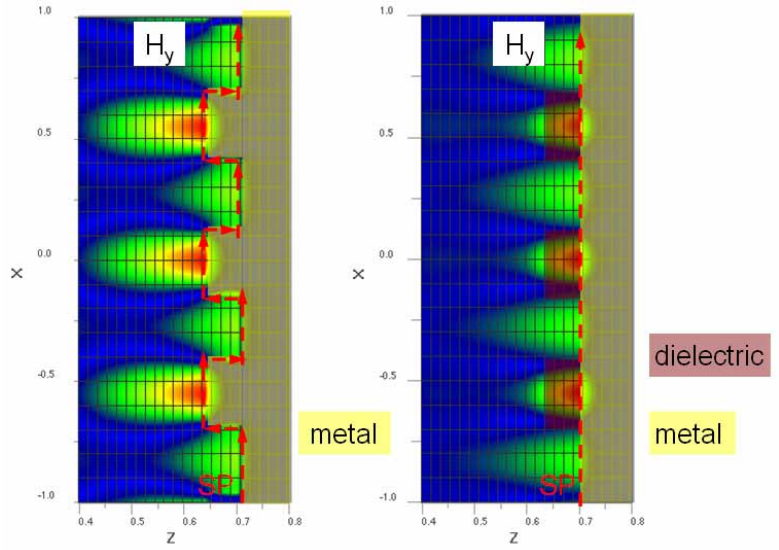

Fig. 8. FDTD simulations of surface plasmon propagation path for a MM structure (left) and a DM structure (right).

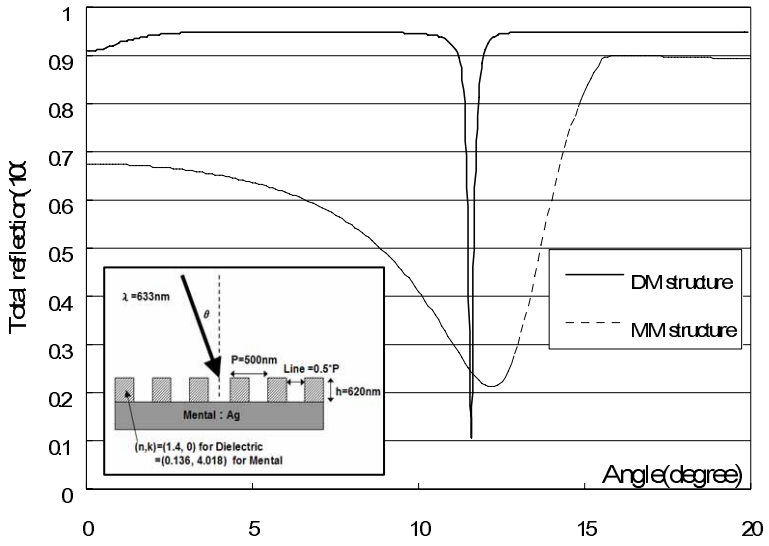

Fig. 9. RCWA simulation of DM and MM structures. (Simulation parameters are detailed)

#10399 - $15.00 USD Received 31 January 2006; revised 29 March 2006; accepted 30 March 2006

6. Conclusions

In this article, we demonstrated that a subwavelength metal slit surrounded by dielectric surface gratings can also possess a directional beaming effect. We proposed that a surface plasmon diffraction scheme can be used to explain three kinds of beaming conditions (positive angle, negative angle and zero degree). All simulations are consistent and in agreement with the experimental results. By comparing MM structures to DM structures, we found that DM structures offer better performance and have the advantage of being able to be more readily mass produced for industrial applications. With the benefits of controlling light in a microscopic world, this new mechanism as disclosed in this article has the potential to be integrated with other fields such as nanolithography [8-9], optical storage [10], optical communication, and biosensors [11].

Acknowledgments

We deeply appreciate the support from the "Nano-writer and Sub-wavelength Surface Structure Design for Optical Applications" a project funded by the Materials Research Laboratory, Industrial Technology Research Institute (ITRI), Taiwan. We also appreciate the E-beam lithography system support by the Center for Information and Electronics Technologies, National Taiwan University. The authors would also like to acknowledge the financial support of this research from the National Science Council of Taiwan, through Grants NSC 93-2622-E-002-003.

#10399 - $15.00 USD Received 31 January 2006; revised 29 March 2006; accepted 30 March 2006